Chemistry, Physics and Technology of Surface. 2021. V. 12. N 4. P. 283-290

UDC 544.228 : 544.18 (54-31) doi: 10.15407/hftp12.04.283

O.V. Filonenko, A.G. Grebenyuk, V.V. Lobanov

QUANTUM CHEMICAL MODELING OF THE STRUCTURE AND PROPERTIES OF SnO_2 NANOCLUSTERS

Chuiko Institute of Surface Chemistry of National Academy of Sciences of Ukraine
17 General Naumov Str., Kyiv, 03164, Ukraine, E-mail: filonenko_ov@ukr.net

By the method of density functional theory with exchange-correlation functional B3LYP and basis set 3-21G (d), the structural and energy characteristics have been considered of the molecular models of SnO_2 nanoclusters of different size and composition with the number of Sn atoms from 1 to 10. Incompletely coordinated surface tin atoms were terminated by hydroxyl groups. It has been shown that the Sn–O bond length in nanoclusters does not depend on the cluster size and on the coordination number of Sn atoms, but is determined by the coordination type of neighboring oxygen atoms. Namely, the bond length $Sn–O^{(3)}$ (≅ 2.10 Å) is greater than that of $Sn–O^{(2)}$ (≅ 1.98 Å). The calculated values of $Sn–O^{(3)}$ bond lengths agree well with the experimental ones for crystalline SnO_2 samples (2.05 Å). The theoretically calculated width of the energy gap decreases naturally with increasing cluster size (from 6.14 to 3.46 eV) and approaches the experimental value of the band gap of the SnO_2 crystal (3.6 eV). The principle of additivity was used to analyze the energy characteristics of the considered models and to estimate the corresponding values for a cassiterite crystal. According to this principle, a molecular model can be represented as a set of atoms or atomic groups of several types that differ in the coordination environment and, therefore, make different contributions to the total energy of the system. The calculated value of the atomization energy for SnO_2 is 1661 kJ/mol and corresponds satisfactorily to the experimentally measured specific atomization energy of crystalline SnO_2 (1381 kJ/mol). It has been shown that a satisfactory reproduction of the experimental characteristics of crystalline tin dioxide is possible when using clusters containing at least 10 state atoms, for example, $(SnO_2)_{10}·14H_2O$.

***Keywords**: SnO_2 crystal structure, solid state thermochemistry, density functional theory, cluster model*

INTRODUCTION

Tin dioxide is the most common and most thermodynamically stable among tin oxides (enthalpy of formation $\Delta H^0_{298} = –581$ kJ/mol) [1, 2]. Under normal conditions, tin(IV) oxide crystallizes in the tetragonal structure of rutile with lattice parameters $a = 4.737$ Å, $c = 3.186$ Å (spatial group $P4_2/mnm$). For SnO_2, this is only one stable phase. In the nature it occurs as a mineral cassiterite [2].

The SnO_2 unit cell consists of two formula units. Each tin atom is six-coordinated, its coordination environment is almost a regular octahedron (Fig. 1). The four oxygen atoms (equatorial) lie in the same plane and have shorter Sn–O bonds (1.98 Å), the other two bonds are slightly longer and are axial (2.1 Å). Oxygen atoms are tricoordinated. SnO_6 octahedra combine into chains elongated along the crystallographic direction *c*. Each SnO_6 octahedron has two common edges with ajacent octahedra [2, 3].

The crystalline tin(IV) oxide is a wide-band *n*-type semiconductor with a band gap of 3.6 eV [1, 3]. It is characterized by low electrical resistance ($3.4·10^3$ Ohm/cm) [4], high optical transparency in the visible region of the spectrum [5] and chemical stability at high temperatures [6]. Although SnO_2 is transparent in the visible range, it has a high reflectivity in the infrared range [3].

Real SnO_2 crystals contain various bulk and surface defects, mostly due to oxygen deficiency, which leads to the formation of regions corresponding to the lower oxides of Sn_3O_4 and SnO [3]. In most cases, a tin atom exhibits two possible oxidation states: Sn^{2+} and Sn^{4+} (the latter is more stable), and oxides of SnO and SnO_2 are formed, respectively. The capability of tin atoms to be in two oxidation states determines the redox properties of the SnO_2 surface. Reduction of Sn(+4) to Sn(+2) can occur quite easily either due to chemisorption of donor molecules, or due to the capture of electrons released by the lattice anions during the formation of an oxygen vacancy [7]. A change in the composition of the oxide causes a change in the conductivity that can be measured. This is a

basis for the use of tin dioxide in the production of gas sensors, in which it is used in the form of polycrystalline powder [8–10].

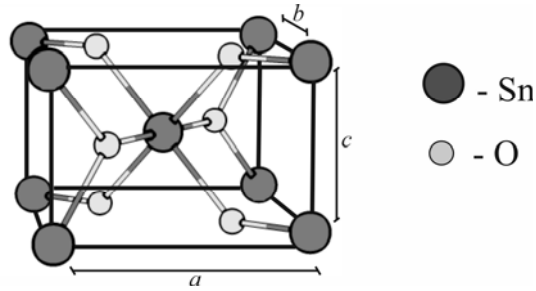

Fig. 1. The structure of the SnO_2 unit cell [3]

Tin dioxide is one of the classic materials, the research of which has remained promising for more than a decade. The wide range of applications of SnO_2-based materials is due to a combination of a number of unique optical and electrophysical properties.

In addition, such materials are non-toxic and cost-effective. Thus, SnO_2 is widely used as an anode material in lithium-ion batteries [11, 12], a catalyst for the oxidation of organic compounds [13–15], transparent electrodes of solar panels, LEDs, various electronic and optical coatings [16–19].

To date, tin dioxide, as a bulk (3D) material, is quite well studied. However, different nanostructured types of SnO_2 show better properties compared to bulk types for both gas analysis and a wide range of other applications. As shown in [20–22], the chemical and electrophysical properties of tin dioxide in the nanocrystalline state significantly depend on the particle size. Thus, in [23] the values of the band gap for nanoscale and filamentous nanostructures are determined, which are in the range from 3.85 to 4.2 eV and from 2.8 to 3.4 eV, respectively. Nanosized powders are characterized by slightly inflated values of the band gap, and for filamentous structures, the value of the band gap is slightly lower compared to the value characteristic of crystalline samples of cassiterite (3.6 eV).

A large number of incompletely coordinated atoms on the surface significantly changes the physical and chemical properties of low-size oxide materials compared to their bulk counterparts. During the transition to nanoscale, with the increase of the specific surface on which Sn(4+) and Sn(2+) ions coexist, the unique redox properties of the SnO_2 surface intensify. As a result, nanosized oxide materials, such as nanoparticles, nanospheres, nanotubes, nanowires, nanobands are of great interest [3].

Various applications of tin dioxide have led to the interest of researchers in the construction and systematic analysis of the properties of theoretical models for crystals and nanoparticles of this substance to study the dependence of structure - properties, in particular with the use of quantum chemistry [24]. Periodic [25–29] and cluster [30–34] approaches to modeling the structure and properties of SnO_2 are known in the literature. The latter are more convenient for reproducing properties of the nanoparticles of tin dioxide, because they do not have a long-range order. Cluster models are based on the capability to model a crystal or its surface with a small number of atoms that form it. The use of cluster models allows one the use of powerful computer programs designed to calculate the properties of molecules, but require careful selection of a molecular cluster itself. The results obtained using a cluster model depend on the size of the cluster, its stoichiometry and shape.

Based on the methods of computer modeling of the surface of the tin dioxide [1, 3, 28, 29], a row of the catalytic activity of its faces has been proposed, namely: (110) < (001) < (100) < (101). It is known [3] that the face (110) is the most stable in oxides with the structure of rutile, and makes up most of the surface area of crystalline samples.

Using computer simulation methods that use periodic boundary conditions, the types are examined of structural defects that can be formed on the surface of tin dioxide. Thus, in [26], within the method of density functional theory, it has been found that oxygen vacancies are the main cause of *n*-type conductivity due to the formation of donor levels on the bottom of the conduction band due to the transition of electrons from Sn(II) to Sn(IV) sites. This applies to oxygen vacancies, which can be found both in the bulk of the crystal and on its surface. The energy of formation of oxygen vacancies in SnO_2 is very small, so such defects are formed relatively easily [29].

In [25], the bulk properties of the cassiterite crystal and the properties of (100), (110), (001), (101) SnO_2 surfaces, both pure and with water molecules adsorbed on them, were studied by the density functional theory method with imposition of periodic boundary conditions. It is

shown that dissociative adsorption of water molecules is the most favorable for all considered faces of SnO_2.

The process of doping of the tin dioxide (110) surface with Co, Cu, and Zn atoms was studied in [30] within the framework of a cluster approach. When modeling the stoichiometric surface, the $Sn_{15}O_{30}$ cluster was chosen, whereas the $Sn_{15}O_{29}$ and $Sn_{15}O_{28}$ clusters were selected for the reconstructed surface. It has been shown that in the transition from an oxidized surface to a reduced one, the absence of bridged oxygen atoms generates electron levels in the band gap due to 5*s*/5*p* orbitals of four- and five-coordinated Sn atoms and 2*p* orbitals of O atoms placed on the surface. The process of addition of Co atoms is exothermic, while addition of Cu and Zn atoms is endothermic.

Using the $Sn_{10}O_{16}$ cluster as a surface tin dioxide model, its interaction with a formaldehyde molecule and the process of its partial oxidation at different temperatures were studied. Analysis of the results of calculations of SnO_2 clusters with different functionals has shown that the most acceptable functional is B3LYP [34].

The paper considers molecular models of SnO_2 of different size and composition with the number of Sn atoms from 1 to 10. The results obtained for these models are compared with the available in the literature experimental data.

COMPUTATIONAL METHOD

The calculations were performed by the method of density functional theory with the exchange-correlation functional B3LYP [35–37] and the basis set 3-21G(d) within the PC GAMESS software package (FireFly 8.2.0). In [34] it was shown that the use of this method with this functional gives results that are in good agreement with the experimental ones in the calculation of the atomic and electronic structure of a number of crystalline oxides, in particular tin dioxide.

The equilibrium spatial structures of the original clusters and adsorption complexes were found by minimizing the norm of the total energy gradient.

RESULTS AND DISCUSSION

The equilibrium structures of the considered SnO_2 cluster models are shown in Fig. 2. The simplest model is molecule of tin(IV) hydroxide – $Sn(OH)_4$ (Fig. 2 *a*). The cluster has a tetrahedral configuration. The Sn atom is four-coordinated, and the four oxygen atoms associated with it are two-coordinated. The length of the $Sn^{(4)}–O^{(2)}$ bonds is 1.96 Å. This cluster cannot describe all the structural properties of a cassiterite crystal, because the coordination number of a tin atom in it is only 4, and not 6, as in a crystal. When two $Sn(OH)_4$ molecules combine into a coordination dimer (Fig. 2 *b*), a cluster of $(SnO_2)_2{\cdot}4H_2O$ is formed, in which two Sn atoms become five-coordinated and oxygen atoms of two hydroxyl groups become tricoordinated. This leads to the elongation of the $Sn^{(5)}–O^{(3)}$ bonds, which are 2.08 and 2.14 Å. The presence of two values of bond lengths in the formed cycle indicates the molecular properties of the model. Molecular models are structures in which individual molecules can be distinguished in a cluster based on the difference between intramolecular and intermolecular bonds, which are usually longer. Unlike molecular models, polyhedral models cannot separate individual molecules because the bond lengths between the same types of atoms are identical.

A further increase in the size of the model leads to the formation of the structure $(SnO_2)_4{\cdot}6H_2O$ in which two tin atoms acquire an octahedral configuration (Fig. 2 *c*), i.e. the coordination number becomes equal to 6, which corresponds to the structure of the SnO_2 crystal. The lengths of the $Sn^{(6)}–O^{(3)}$ bonds average 2.13 Å, and the average length of the $Sn^{(5)}–O^{(3)}$ bonds is slightly smaller – 2.07 Å. Two types of clusters with 6 tin atoms are considered. Both clusters are characterized by the same quantitative composition, they correspond to the gross formula $(SnO_2)_6{\cdot}12H_2O$, but their structures are different. The cluster (Fig. 2 *d*) has a chain structure in which four tin atoms are six-coordinated, two edge tin atoms are five-coordinated. The lengths of the $Sn^{(6)}–O^{(3)}$ bonds average 2.12 Å, and the average length of the $Sn^{(5)}–O^{(3)}$ bonds is slightly smaller – 2.10 Å. The second type corresponds to a cluster with a ring-shaped structure, in which all tin atoms are six-coordinated (Fig. 2 *e*). The average length of $Sn^{(6)}–O^{(3)}$ bonds is 2.15 Å. The cluster with a ring-like structure is thermodynamically more advantageous than that with a chain structure. The largest cluster $(SnO_2)_{10}{\cdot}14H_2O$ we

considered contains 10 tin atoms, eight of which are six-coordinated (Fig. 2 *f*). The average length of $Sn^{(6)}$–$O^{(3)}$ bonds is 2.14 Å, and the $Sn^{(5)}$–$O^{(3)}$ bonds are 2.04 Å.

For all the clusters considered in the work, the average bond length $Sn^{(5, 6)}$–$O^{(2)}$ is 1.97 Å.

An analysis of the obtained structural parameters of clusters shows that the Sn–O bond length does not depend on the cluster size and the coordination number of Sn atoms, but depends on the type of neighboring oxygen atoms (two- or tricoordinated) the tin atom is connected to. Namely, the bond length Sn–$O^{(3)}$ (≅ 2.10 Å) > the bond length Sn–$O^{(2)}$ (≅ 1.98 Å). The obtained Sn–$O^{(3)}$ bond lengths agree well with the experimental values for crystalline SnO_2 samples (2.05 Å). For nanoparticles, the experimentally measured bond lengths range from 1.91 to 2.16 Å.

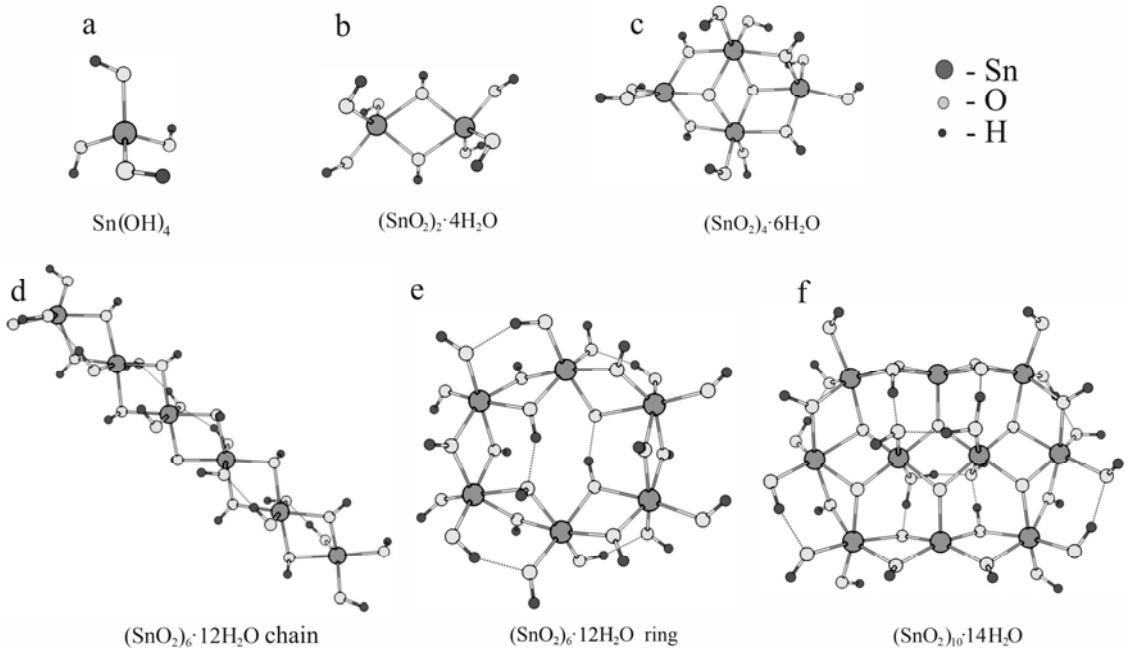

Fig. 2. Equilibrium spatial structures of the SnO_2 molecular models of different size and composition (N_{Sn} = 1, 2, 4, 6, 10)

Table. Bond lengths (Å) of the equilibrium SnO_2 molecular models of different size and composition (N_{Sn} = 1, 2, 4, 6, 10)

	$Sn(OH)_4$	**$(SnO_2)_2$· ·$4H_2O$**	**$(SnO_2)_4$· ·$6H_2O$**	**$(SnO_2)_6$· ·$12H_2O$ ring**	**$(SnO_2)_6$· ·$12H_2O$ chain**	**$(SnO_2)_{10}$· ·$14H_2O$**	**exp.**
d **($Sn^{(4)}$ – $O^{(2)}$)**	1.96						
d **($Sn^{(5)}$ – $O^{(2)}$)**		1.97	1.97		1.96		
d **($Sn^{(5)}$ – $O^{(3)}$)**		2.10	2.06		2.10	2.01	
d **($Sn^{(6)}$ – $O^{(2)}$)**			1.98	1.98	1.97	1.99	
d ($Sn^{(6)}$ – $O^{(3)}$)			2.15	2.15	2.14	2.20	2.05 (cryst.) 1.96–2.16 (nanopart.)
E**(LUMO) – -*****E*****(HOMO)**	6.48	6.14	5.06	5.52	4.42	3.46	3.6 (cryst.)

Based on the results of calculations, we can assume that the larger values of the lengths correspond to the Sn–O bonds in the bulk, and the smaller ones - to the peripheral Sn–O bonds, *i.e.* in which the tin atoms are bound to the surface OH groups.

The principle of additivity, developed first for organic substances [38] and then adapted for

crystals of inorganic substances taking into account the different coordination environment of atoms inside and on the surface of cluster models [39], was used to analyze the energy characteristics of the considered models and to estimate the corresponding values for the cassiterite crystal. According to this principle, a molecular model can be represented as a set of atoms or atomic groups of several types, which differ in the coordination environment and, therefore, make different contributions to the system energy [40]. Since in a molecular model, in contrast to the simulated crystal, there are always surface (terminal) atoms with reduced coordination numbers, to determine the energy characteristics of the formula unit of the crystal it is necessary to use at least two (or more) molecular models that differ in their coordination composition for a quantity, a multiple of the formula unit of the crystal.

The cluster $(SnO_2)_{10}\cdot 14H_2O \equiv 8Sn^{VI}2Sn^{V}18O^{III}16O^{II}28H$ includes eight hexa- and two five-coordinated tin atoms, eighteen tricoordinated and sixteen double-coordinated oxygen atoms. According to the principle of additivity, to calculate the energy of the formula unit SnO_2, one has to subtract the energy of the cluster $(SnO_2)_2\cdot 4H_2O \equiv 2Sn^{V}2O^{III}6O^{II}8H$, consisting of two five-coordinated tin atoms and two tricoordinated and six two-coordinated oxygen atoms to obtain ($8Sn^{VI}16O^{III}10O^{II}20H \equiv (SnO_2)_8\cdot 10H_2O$), inherent in the crystal (see formula 1).

$$\begin{array}{l} 8Sn^{(6)}2Sn^{(5)}18O^{(3)}16O^{(2)}28H \\ \quad 2Sn^{(5)}2O^{(3)}6O^{(2)}8H \\ \hline 8Sn(5)16O(3)10O(2)20H \end{array} \quad (1)$$

.

The energy of the formula unit ($E_{tot(SnO_2)}$) was found according to the formula (2):

$$E_{tot(SnO_2)} = [E((SnO_2)_{10}\cdot 14H_2O) - -E((SnO_2)_2\cdot 4H_2O) - 10\,E(H_2O)] / 8, \quad (2)$$

where $E((SnO_2)_{10}\cdot 14H_2O)$, $E((SnO_2)_2\cdot 4H_2O)$ and $E(H_2O)$ – total energies of optimized structures at 0 K.

The value of atomization energy (E_{at}) for SnO_2 was calculated by formula (3):

$$E_{at} = (E_{tot(Sn)} + 2E_{tot(O)}) - E_{tot(SnO_2)} \quad (3)$$

where $E_{tot(Sn)}$, $E_{tot(O)}$ are the total energies of the tin and oxygen atoms in the triplet state, respectively, and the total energy of the formula unit of tin dioxide.

The calculated value is 1661 kJ/mol and satisfactorily corresponds to the experimentally measured specific atomization energy of crystalline SnO_2 (1381 kJ/mol).

For tin dioxide clusters, the energy gap is theoretically calculated as the energy difference between the lower vacant molecular orbital and the higher occupied orbital. As the cluster size increases, the energy gap naturally decreases from 6.48 eV for $Sn(OH)_4$ to 3.46 eV for $(SnO_2)_{10}\cdot 14H_2O$ (see Table) and approaches the experimental value of the band gap for the SnO_2 crystal (3.6 eV).

CONCLUSION

A set of molecular models for tin dioxide crystals has been designed due to association and condensation of several (from 1 to 10) $Sn(OH)_4$ molecules. Their geometry and energy characteristics have been simulated within density functional theory. From the results of calculations it follows that satisfactory reproduction of the experimental characteristics of crystalline tin dioxide is possible when using clusters containing at least 10 tin atoms.

Квантовохімічне моделювання структури та властивостей нанокластерів SnO_2

О.В. Філоненко, А.Г. Гребенюк, В.В. Лобанов

Інститут хімії поверхні ім. О.О. Чуйка Національної академії наук України
вул. Генерала Наумова, 17, Київ, 03164, Україна, filonenko_ov@ukr.net

Методом теорії функціоналу густини з обмінно-кореляційним функціоналом B3LYP і базисним набором 3-21G(d) розглянуто структурні та енергетичні характеристики молекулярних моделей нанокластерів SnO_2 різного розміру та складу з кількістю атомів Sn від 1 до 10. Поверхневі неповнокоординовані атоми Стануму замикались гідроксильними групами. Показано, що довжина зв'язку Sn–O в нанокластерах не залежить від їхнього розміру та координаційного числа атомів Sn, а визначається координаційним типом сусідніх атомів Оксигену. А саме, довжина зв'язку $Sn–O^{(3)}$ (≅ 2.10 Å) > довжини зв'язку $Sn–O^{(2)}$ (≅ 1.98 Å). Одержані довжини зв'язку $Sn–O^{(3)}$ добре узгоджуються із експериментальними значеннями для кристалічних зразків SnO_2 (2.05 Å). Теоретично розрахована ширина енергетичної щілини із збільшенням розміру кластера закономірно зменшується (від 6.14 до 3.46 еВ) і наближається до експериментального значення ширини забороненої зони кристала SnO_2 (3.6 еВ). Для аналізу енергетичних характеристик розглянутих моделей та оцінки відповідних величин для кристала каситериту використано принцип адитивності. Згідно цього принципу, молекулярна модель може бути представлена як сукупність атомів або атомних угруповань декількох типів, які різняться координаційним оточенням і, отже, дають різні внески в повну енергію системи. Розрахована енергія атомізації для SnO_2 складає 1661 кДж/моль і задовільно відповідає експериментально виміряній питомій енергії атомізації кристалічного SnO_2 (1381 кДж/моль). Показано, що задовільне відтворення екпериментальних характеристик кристалічного діоксиду олова можливе при використанні кластерів, які містять щонайменше 10 атомів Стануму, наприклад, $(SnO_2)_{10}·14H_2O$.

***Ключові слова**: кристалічна структура SnO_2, термохімія твердого тіла, теорія функціоналу густини, кластерна модель*

REFERENCES

1. Batzill M., Diebold U. The surface and materials science of tin oxide. *Prog. Surf. Sci*. 2005. **79**(2–4): 47.
2. Mallika C., Edwin Suresh Raj A.M., Nagaraja K.S., Sreedharan O.M. Use of SnO for the determination of standard Gibbs energy of formation of SnO_2 by oxide electrolyte e.m.f. measurements. *Thermochim. Acta*. 2001. **371**(1–2): 95.
3. *Tin Oxide Materials. Synthesis, Properties, and Applications*. (Elsevier Inc., 2020).
4. Sidorenko T.V., Poluyanska V.V. Tin dioxide: structure, properties, applications and prospects for further study of its capillary properties. *Adhesion of melts and soldering of mater*. 2015. **48**: 15. [in Ukrainian].
5. Sanon G., Rup R., Mansingh A. Band-gap narrowing and band structure in degenerate tin oxide (SnO_2) films. *Phys. Rev. B. Condens Matter*. 1991. **44**(11): 5672.
6. Tan L., Wang L., Wang Y. Hydrothermal synthesis of SnO_2 nanostructures with different morphologies and their optical properties. *J. Nanomater*. 2011. **2011**(23): 1.
7. Zheleznyak A.R., Bakalinskaya O.M., Brychka A.V., Kalenyuk G.O., Kartel M.T. Properties, methods of obtaining and applying nanoxide of stanum. *Surface*. 2020. **12(27)**: 193. [in Ukrainian].
8. Das S., Jayaraman V. SnO_2: A comprehensive review on structures and gas sensors. *Prog. Mater. Sci.* 2014. **66**: 112.
9. Yang J.W., Cho H.J., Lee S.H., Lee J.Y. Characterization of SnO_2 ceramic gas sensor for exhaust gas monitoring of SVE process. *Environ. Monit. Assess.* 2004. **92**(1–3): 153.
10. Suman P.H., Felix A.A., Tuller H.L., Varela J.A., Orlandi M.O. Comparative gas sensor response of SnO_2, SnO and Sn_3O_4 nanobelts to NO_2 and potential interferents. *Sensors Actuators B Chem*. 2015. **208**: 122.
11. Lee S.-Y., Park K.-Y., Kim W.-S., Yoon S., Hong S.-H., Kang K., Kim M. Unveiling origin of additional capacity of SnO_2 anode in lithium-ion batteries by realistic *ex situ* TEM analysis. *Nano Energy*. 2016. **19**: 234.
12. Odani A., Nimberger A., Markovsky B., Sominski E., Levi E., Kumar V.G. Development and testing of nanomaterials for rechargeable lithium batteries. *J. Power Sources*. 2003. **119–121**: 517.

13. Xu X., Zhang R., Zeng X., Han X., Li Y., Liu Y., Wang X. Effects of La, Ce, and Y oxides on SnO_2 catalysts for CO and CH_4 oxidation. *Chem. Cat. Chem*. 2013. **5**(7): 2025.
14. Liberkova K., Touroude R. Performance of Pt/SnO_2 catalyst in the gas phase hydrogenation of crotonaldehyde. *J. Mol. Catal. A Chem*. 2002 **180**(1): 221.
15. Manjunathan P., Marakatti V.S., Chandra P., Kulal A.B., Umbarkar S.B., Ravishankar R. Mesoporous tin oxide: an efficient catalyst with versatile applications in acid and oxidation catalysis. *Catal. Today*. 2018. **309**: 61.
16. Ray S., Dutta J., Barua A.K. Bilayer SnO_2: In/SnO_2 thin films as transparent electrodes of amorphous silicon solar cells. *Thin Solid Films*. 1991. **199**(2): 201.
17. Tran V.-H., Ambade R.B., Ambade S.B., Lee S.-H., Lee I.-H. Low-temperature solution-processed SnO_2 nanoparticles as a cathode buffer layer for inverted organic solar cells. *ACS Appl. Mater. Interfaces*. 2017. **9**(2): 1645.
18. Valitova I., Natile M.M., Soavi F., Santato C., Cicoira F. Tin dioxide electrolyte-gated transistors working in depletion and enhancement modes. *ACS Appl. Mater. Interfaces*. 2017. **9**(42): 37013.
19. Granqvist C.G. Transparent conductors as solar energy materials: A panoramic review. *Sol. Energy Mater. Sol. Cells*. 2007. **91**(17): 1529.
20. Luo S., Fan J., Liu W., Zhang M., Song Z., Lin C., Wu X., Chu P.K. Synthesis and low-temperature photoluminescence properties of SnO_2 nanowires and nanobelts. *Nanotechnology.* 2006. **17**(6): 1695.
21. Jin Z., Fei G.T., Cao X.L., Wang X.W. Fabrication and optical properties of mesoporous SnO_2 nanowire arrays. *J. Nanosci. Nanotechnol*. 2010. **10**(8): 5471.
22. Zhang Z., Gao J., Wong L.M., Tao J.G., Liao L., Zheng Z., Xing G.Z., Peng H.Y., Yu T., Shen Z.X., Huan C.H., Wang S.J., Wu T. Morphology-controlled synthesis and a comparative study of the physical properties of SnO_2 nanostructures: from ultrathin nanowires to ultrawide nanobelts. *Nanotechnology*. 2009. **20**(13): 135605.
23. Nagirnyak S.V. Ph.D (Technology of inorganic substances) Thesis. (Kyiv, 2018). [in Ukrainian].
24. Sauer J. Molecular models in ab initio studies of solids and surfaces: from ionic crystals and semiconductors to catalysts. *Chem. Rev.* 1989. **89** (1): 199.
25. Oviedo J., Gillan M.J. Energetics and structure of stoichiometric SnO_2 surfaces studied by first-principles calculations. *Surf. Sci*. 2000. **463**(2): 93.
26. Hong S.-N., Kye Y.-H., Yu C.-J., Jong U.-G., Ri G.-C., Choe C.-S., Han J.-M. Ab initio thermodynamic study of the SnO_2 (110) surface in an O_2 and NO environment: a fundamental understanding of the gas sensing mechanism for NO and NO_2. *Phys. Chem. Chem. Phys*. 2016. **18**(46): 31566.
27. Agamalyan M.A., Hunanyan A.A., Harutyunyan V.M., Aleksanyan M.S., Sayunts A.G., Zakaryan A.A. Studies of the interaction of H_2O_2 with the SnO_2 (110) surface from first principles. *Izvestia of the National Academy of Sciences of Armenia, Phys*. 2020. **55**(3): 358. [in Russian].
28. Korotcenkov G., Golovanov V., Brinzari V., Cornet A., Morante J., Ivanov M. Distinguishing feature of metal oxide films' structural engineering for gas sensor applications. *J. Phys*. 2005. **15**(1): 256.
29. Kılıç C., Zunger A. Origins of coexistence of conductivity and transparency in SnO_2. *Phys. Rev. Lett*. 2002. **88**(9): 95.
30. Sensato F.R., Filho O.T., Longo E., Sambrano J.R., Andres J. Theoretical analysis of the energy levels indused by oxygen vacancies and the doping process (Co, Cu and Zn) on SnO_2 (110) surface models. *J. Mol. Struct*. 2001. **541**(1–3): 69.
31. Abdulsattar M.A., Abed H.H., Jabbar R.H., Almaroof N.M. Effect of formaldehyde properties on SnO_2 clusters gas sensitivity: A DFT study. *J. Mol. Graphics Modell.* 2021. **102**: 107791.
32. Zhao Z., Li Z. First-principle calculations on the structures and electronic properties of the CO-adsorbed $(SnO_2)_2$ clusters. *Struct. Chem*. 2020. **31**(5): 1861.
33. Ducere J.-M., Hemeryck A., Esteve A., Rouhani M.D., Landa G., Menini P., Tropis C., Maisonnat A., Fau P., Chaudret B. A Computational chemist approach to gas sensors: modeling the response of SnO_2 to CO, O_2, and H_2O gases. *J. Comput. Chem*. 2011. **33**(3): 247.
34. Tingting S., Fuchun Z., Weihu Z. Density functional theory study on the electronic structure and optical properties of SnO_2. *Rare Metal Materials and Engineering*. 2015. **44**(10): 2409.
35. Muscat J., Wander A., Harrison N.M. On the prediction of band gaps from hybrid functional theory. *Chem. Phys. Lett*. 2001. **342**(3–4): 397.
36. Perdew J.P., Wang Y. Accurate and simple analytic representation of the electron-gas correlation energy. *Phys. Rev. B*. 1992. **45**(23): 13244.
37. Lee C., Yang R.G., Parr R.G. Development of the Colle-Salvetti correlation-energy formula into a functional of the electron density. *Phys. Rev. B*. 1988. **37**(2): 785.
38. Cohen N., Benson S.W. Estimation of heats of formation of organic compounds by additivity methods. *Chem. Rev*. 1993. **93**(7): 2419.

39. Grebenyuk A.G., Zaets V.A., Gorlov Yu.I. Application of the MINDO/3 and MNDO methods to the calculation of the enthalpy of formation of solids. *Ukrainian Chemistry Journal*. 1995. **61**(9): 23.
40. Reznitsky L.A. *Chemical bond and transformation of oxides*. (Moscow: Publishing house of Moscow State University, 1991).

Received 01.07.2021, accepted 01.12.2021